

Microstructure and Properties of Electrodeposited Ni-CeO₂ Coatings

Chao Xiong^{1,2}, Yuxin Wang^{2,*}, Bo Hu², Lei Chen¹, See Leng Tay², Ancheng Xu^{1,3,*}, Wei Gao²

¹School of Electrical and Photoelectric Engineering, Changzhou Institute of Technology, Changzhou, 213002 China

²Department of Chemical & Materials Engineering, the University of Auckland, PB 92019, Auckland 1142, New Zealand

³State Key Laboratory of Functional Materials for Informatics, Shanghai Institute of Microsystem and Information Technology, Chinese Academy of Sciences, 865 Changning Road, Shanghai 200050, China

*E-mail: ywan943@aucklanduni.ac.nz, xiongchaexc88@163.com

Received: 6 November 2015 / Accepted: 1 December 2015 / Published: 1 January 2016

Ni-CeO₂ nano-composite coatings were prepared by electroplating on mild steel from bright nickel solution with dispersed CeO₂ nanoparticles. A systematic study of Ni-CeO₂ coatings with different powder concentrations (CeO₂ concentration = 0-20 g/L) has been conducted. The microstructure of coatings was analyzed using XRD, optical microscope and SEM. The mechanical property including microhardness and wear resistance were measured. It was found that incorporation of CeO₂ particles can decrease the grain size and improves the mechanical properties of Ni coatings. The optimum concentration of CeO₂ powder for the property improvement is 10 g/L. The micro hardness of the coating can reach ~560 HV₁₀₀ compared to 421 HV₁₀₀ of Ni coating. The effect of CeO₂ nanoparticles on the microstructure and mechanical property of coatings was discussed.

Keywords: Electroplating, Composite coatings, Mechanical property

1. INTRODUCTION

Metal composite coatings have been developed for enhancing the surface properties of material such as wear, corrosion and high temperature oxidation resistance in order to decrease the degradation of working parts [1-4]. Ni has widely been used on the surfaces of metal substrates in order to improve their corrosion and wear resistance. Many contributions have been devoted to improve the properties of electrodeposited Ni or Ni alloys, including co-depositing second-phase particles to form

nanocomposite coatings, modifying deposition parameters and using pulse electroplating. Co-deposition of ceramic nanoparticles with metal and alloy phases to form nanocomposites can bring a significant improvement on physical and chemical properties of the coatings [5-9]. To obtain better properties of Ni based nanocomposite coatings, different hard second-phase nanoparticles such as Al_2O_3 , SiC, ZrO_2 and TiO_2 were mixed into the plating solution; and much effort were contributed to optimize the plating process parameters. [10-13].

CeO_2 is an oxide of the rare earth metal cerium which has many superior properties. It has been proven that electrodeposited CeO_2 into metal coatings can significantly improve the wear resistance of the composite coatings. Y.J. Xue et al studied the tribological performance of Ni– CeO_2 composite coatings. Cârâc et al investigated the relationship between microstructure and microhardness of Ni– CeO_2 and Co– CeO_2 composite coatings. However, few investigations have been done on the relationship of CeO_2 content, microstructure and mechanical properties. [14-19].

In the present work, the nanocomposite Ni– CeO_2 coatings was produced onto mild steel by electroplating. The microstructure and mechanical properties of nanocomposite Ni– CeO_2 coatings was studied in comparison of pure Ni coating.

2. EXPERIMENTAL DETAILS

Both Ni and Ni– CeO_2 composite coatings were electroplated onto the mild steel substrate ($20 \times 30 \times 3 \text{ mm}^3$). The steel substrates were mechanically polished using SiC paper to a grit of #1200, then degreased ultrasonically in ethanol. Before electroplating, the specimens were pre-treated in 1 mol/L HCl solution for 2 min at room temperature.

Electrodeposition was carried out using a power resource (MicroStar, DuPR10-1-3). The plating system consists of a mild steel sample as the cathode and a Ni plate as the anode. The plating bath was composed of 250 g L^{-1} $\text{NiSO}_4 \cdot 6\text{H}_2\text{O}$, 40 g L^{-1} $\text{NiCl}_2 \cdot 6\text{H}_2\text{O}$, 35 g L^{-1} H_3BO_3 , certain amount of brightener additives, and CeO_2 nano-particles from 0 to 20 g L^{-1} . The pH value of bath solution was adjusted at 3.5 by using ammonia solution. All plating processes were conducted under a current density of 20 mA cm^{-2} , stirring rate of 500 rpm and bath temperature of 55°C for 30 min. During the experiment, 7 different concentrations of CeO_2 powders from 0 to 20 g/L were chosen in order to achieve the best properties. CeO_2 nano-particles with a mean diameter of 50 nm were dispersed in the electrolyte. For convenient description, Ni- $x \text{ g/L CeO}_2$ ($x = 0, 5, 10, 15, 20$) was used to represent the coatings with different concentration of CeO_2 powder addition.

Vickers microhardness of coating surface was measured using a load of 100 g with a holding time of 15 s. The average of 5 measurements was used as the hardness. Wear property of coatings was tested using a micro-tribometer (Nanovea, USA) in air at room temperature, relative humidity of ~50% under and dry, non-lubricated conditions. All wear tests were performed under a load of 3 N, a sliding speed of 2 m/min and a contact radius of 6 mm for a total sliding distance of 20 m. The wear weight loss was measured by using an electrical balance with $1 \mu\text{g}$ weighing accuracy. The wear track images of the coatings were observed by high-revolution optical microscope.

The coating surface morphologies were analyzed using optical microscopy. The shape and composition of coating cross-section were analyzed using a field emission scanning electron microscope (FESEM) with an energy dispersive spectroscopy (EDS) system. The phase structure of the coatings was characterized by X-ray diffraction (XRD) with Cu K α radiation ($V = 30$ kV, $I = 15$ mA). Diffraction patterns were recorded in the 2θ range from 20 to 80° at a scanning rate of 1° min^{-1} .

3. RESULTS AND DISCUSSION

3.1 Surface and cross-sectional morphologies of coatings

Fig.1 shows the surface morphologies of Ni-x g/L CeO₂ ($x = 0, 5, 10, 15$ and 20 g/L) coatings with different powder addition under the same electro-deposition conditions. The surface of pure Ni coating was found to be smooth and homogeneous, as shown in Fig.1 (a). Figs. 1(b), (c) and (d) present the surfaces morphologies of Ni–CeO₂ coatings with different CeO₂ contents. CeO₂ nanoparticles were incorporated uniformly into the Ni matrix. The increasing black points indicate that the CeO₂ content in Ni substrate rises with increasing CeO₂ concentration in the bath [20]. The size of largest black particle clouds in the Ni–CeO₂ (20 g/L) coating was $\sim 4 \mu\text{m}$. These large black particle clouds could be due to the agglomeration of CeO₂ nanoparticles. With increasing concentration of CeO₂ nano powders in the bath, more obvious agglomeration sites can be seen in the composite coatings. It also can be seen that the surface roughness of coating was increased with increasing CeO₂ concentration in the bath.

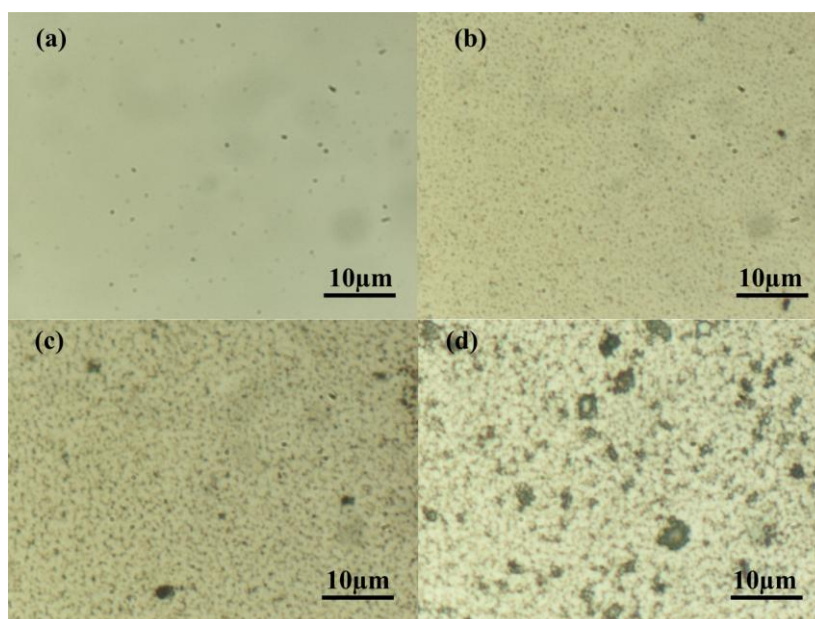


Figure 1. Surface morphologies of electroplating Ni composite coatings: a) Ni coating, b) Ni–CeO₂ (5 g/L), c) Ni–CeO₂ (10 g/L), and d) Ni–TiO₂ (20 g/L) coatings.

The cross-section microstructure of Ni-x g/L CeO₂ coatings was studied by SEM backscatter electron image as shown in Fig.2. A gleaming boundary between the coatings and the steel substrate can be observed. No abruption or cracks exist at the interfaces of the coatings, evidence of a good adhesion between the steel substrate and coating. All coatings have a uniform thickness of ~12.8 μm.

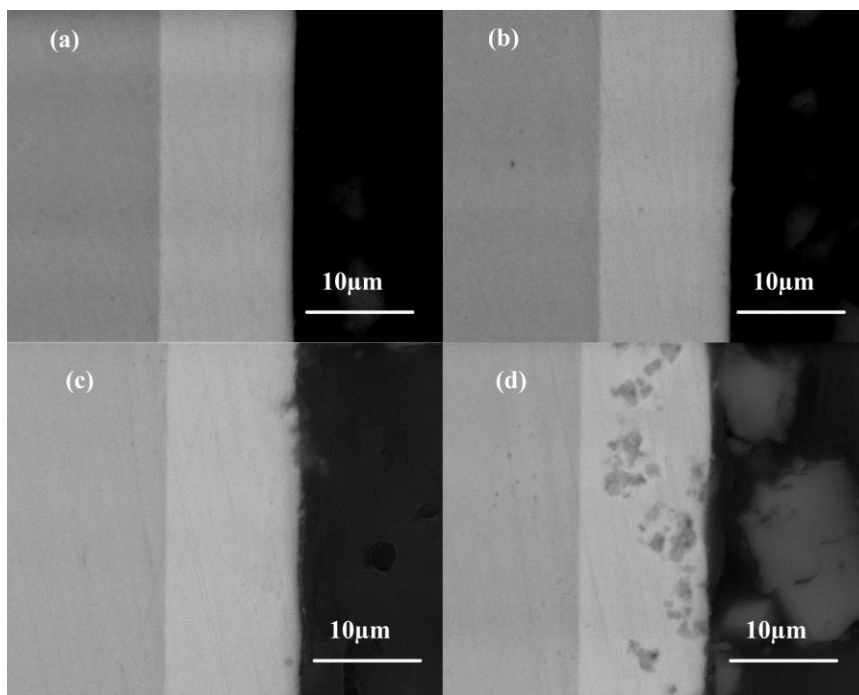


Figure 2. Cross-section SEM images of electroplating Ni coatings: a) Ni coating, b) Ni–CeO₂ (5 g/L), c) Ni–CeO₂ (10 g/L), and d) Ni–TiO₂ (20 g/L) coatings.

No obvious CeO₂ nanoparticles were seen in the cross-section which probably due to their small size and relatively low content as shown in Figs. 2b and 2c. When the amount of CeO₂ nanoparticles addition reaches 20 g/L, obvious CeO₂ particles were seen in the cross-section image which due to the agglomeration of the CeO₂ particles (Fig. 2d). Tiny CeO₂ nanoparticles were aggregated into particle clouds with an average size of about 500 nm or larger and embedded in the Ni coating matrix as second phases during the electroplating process. As the CeO₂ concentration in the bath increases, the corresponding particle clouds in the as-plated coating increases, this is consistent with the grain size analysis and the surface morphology as shown in Table 1 and Fig.1 [21, 22].

3.2 Microstructure of nanocomposite Ni-CeO₂ coatings

Fig.3 illustrates the XRD patterns of electroplated Ni coatings as a function of CeO₂ powder addition. All patterns have a crystalline and face-centered cubic (*fcc*) lattice structure. The predominant planes of the coatings were Ni (111), Ni (200) and Ni (220). The peaks at 65.0° can be assigned to Fe

from the mild steel substrate. No CeO_2 peaks could be detected from the Ni– CeO_2 coatings, probably due to the low quantity of CeO_2 and high intensity of Ni diffraction peaks.

The grain size of the composite coatings was calculated from the measured XRD spectra; and the results are shown in Table 1. The grain sizes vary with the addition of CeO_2 in the plating bath. During the coating formation process, small CeO_2 nanoparticles could provide a large number of nucleation centers and accelerate the deposition rate of coating. Meanwhile, large amount of small particles embedded in the coating hindered the grain growth. Hence the grain sizes were decreased [22]. As the CeO_2 powder concentration in the plating bath increases, the grain size of coating gradually decreases from ~15.4 nm to ~12.3 nm. However, too many nanoparticles would cause agglomeration and emergence of particle clouds. The grain size increases to ~14.5 nm when the CeO_2 concentration of 20g/L.

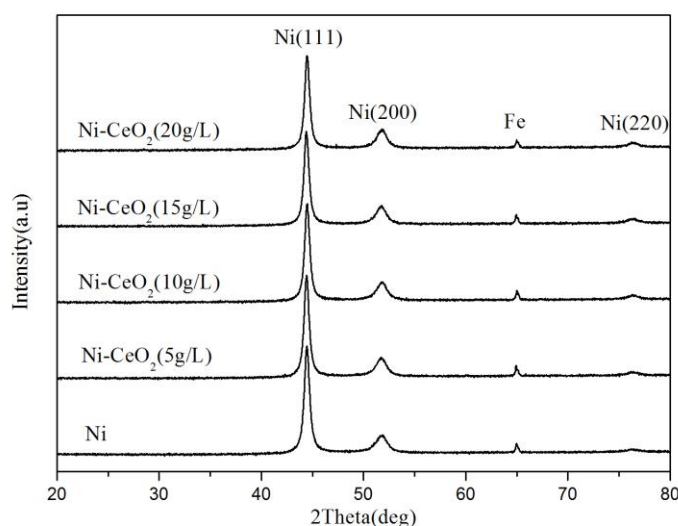


Figure 3. XRD patterns of electroplated nickel composite coatings

Table 1. Grain size of nickel composite coatings electroplated under different conditions

Composition and conditions	Grain size(nm)
Ni coating	15.4±0.1
Ni- CeO_2 (5g/L) composite coating	13.2±0.1
Ni- CeO_2 (10g/L) composite coating	12.3±0.1
Ni- CeO_2 (15g/L) composite coating	12.9±0.1
Ni- CeO_2 (20g/L) composite coating	14.5±0.1

3.3 Microhardness of coatings

The Vickers hardness values of the Ni-CeO₂ composite coatings as a function of the CeO₂ powder concentration in the plating bath are shown in Fig.4. The microhardness of pure Ni coating is ~421 HV. It was increased with increasing CeO₂ content to ~560 Hv for the Ni-10 g/L CeO₂ nanocomposite coating. The improvement of microhardness can be attributed to the combine effect of grain size refining and CeO₂ nanoparticles dispersion strengthening. However, further increasing the amount of CeO₂ concentration leads to more serious particle agglomeration and tends to cause a porosity structure. The microhardness of Ni-20 g/L CeO₂ nanocomposite coating was decreased to ~430 HV, slightly higher than that of pure Ni coating [23].

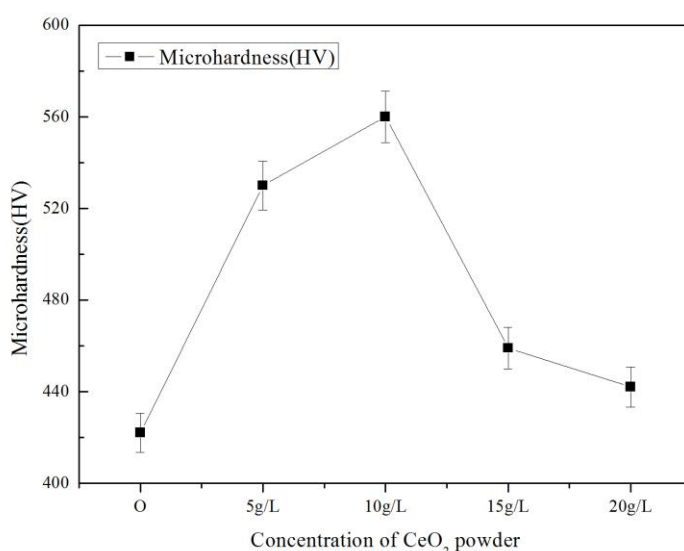


Figure 4. Microhardness of electroplating Ni composite coatings

3.4 Wear property of coatings

The friction coefficient of composite coatings with different CeO₂ powder additions was shown in Fig.5. It can be seen that Ni coating possess the lowest friction coefficient ~ 0.12. With increasing CeO₂ powder concentration, the friction coefficient of coatings first slightly increased, then decreased, and finally increased. The friction coefficients of Ni-x g/L CeO₂ (x = 5, 10, 20 g/L) coatings were about 0.18, 0.15 and 0.24, respectively. The variation of friction coefficient could be attributed to both surface microhardness and roughness of coatings. For the Ni-CeO₂ (5 g/L) coating, the increased friction coefficient mainly comes from to the increasing surface roughness which can be seen in Fig.1. The surface roughness was affected by the embedded hard CeO₂ nanoparticles.

The width of wear track is a direct measure of the wear volume loss, and related to both the hardness and frictional coefficient of coatings. The wear track images of composite coatings were shown in Fig.6. The wear track width of Ni coating, Ni-CeO₂ (5 g/L), Ni-CeO₂ (10 g/L), and Ni-CeO₂

(20 g/L) coatings were ~201, ~192, ~112, and ~165 μm , respectively. These widths first decrease and then increase with the increasing CeO_2 powder concentration in the plating bath, following the same trend of the microhardness as shown in Fig.4, indicating that the hardness played the main role.

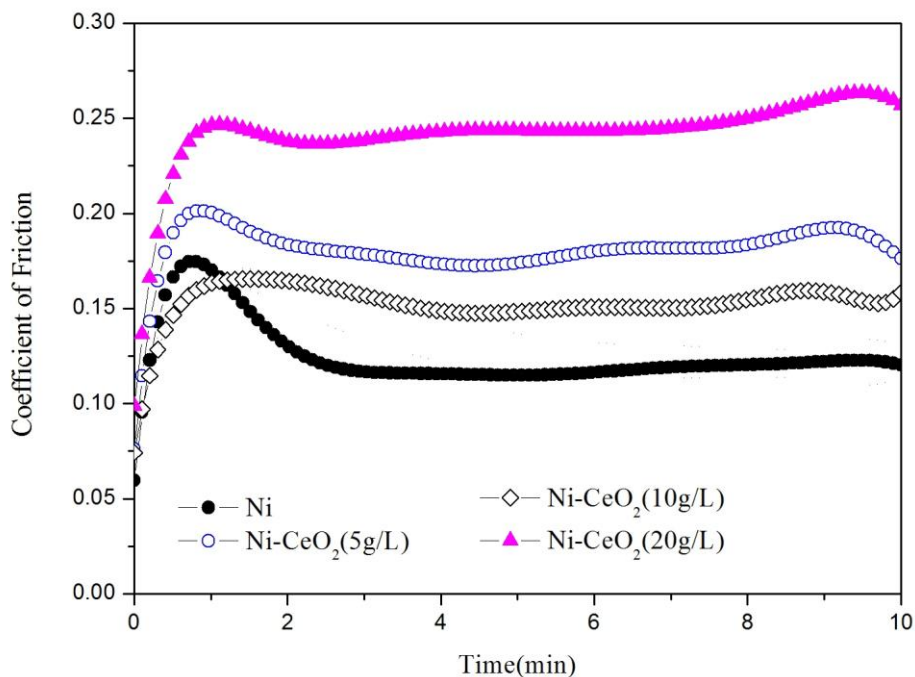


Figure 5. Frictional coefficient curve of nickel composite coatings

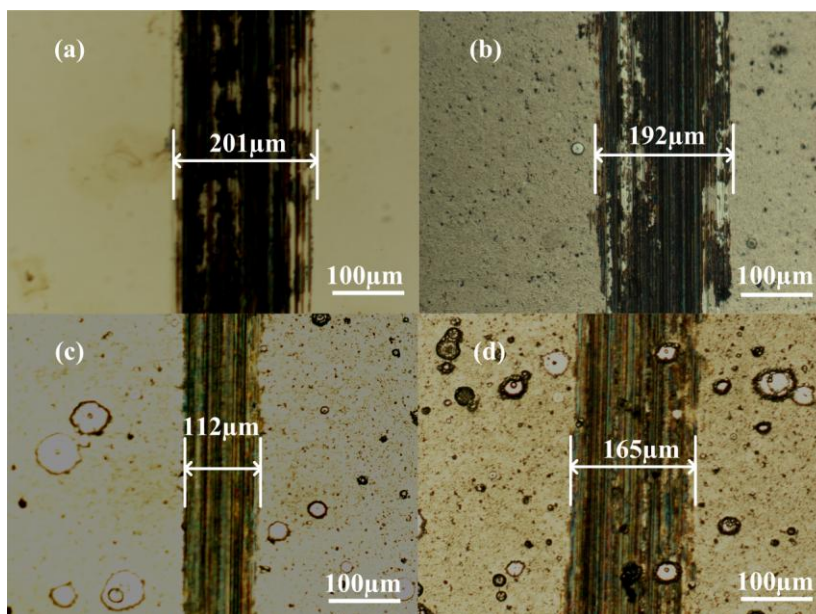


Figure 6. Wear track image of Ni composite coatings: (a) Ni coating, (b) Ni-CeO₂ (5 g/L), (c) Ni-CeO₂ (10 g/L), and (d) Ni-CeO₂ (20 g/L) coatings.

4. CONCLUSIONS

Ni-CeO₂ nanocomposite coatings were prepared by electroplating method. Their microstructure and mechanical properties including microhardness and wear resistance were studied. The microstructure and mechanical properties for the electroplated Ni-CeO₂ nanocomposite coatings is strongly affected by the amount of CeO₂ nanoparticles addition. The incorporation of CeO₂ nanoparticles decreases the grain size of coatings and leads to a dispersion strengthening effect. The mechanical properties of electroplated Ni-CeO₂ coatings reach the optimum value when the CeO₂ concentration is 10 g/L. When the concentration of CeO₂ in the plating bath is more than 10 g/L, deterioration of coating mechanical property occurred due to the porous structure and rough surface of coatings. Further investigations are being carried out in an effort to apply this technology in industrial applications.

ACKNOWLEDGEMENT

The work is supported by the financial support from the China Postdoctoral Science Foundation (No.2013M531849), the Open Project for the Key Laboratory of Jiangsu Provincial Solar-Cell Materials and Technology (No.201202), the Natural Science Foundation of Jiangsu Province (Grant No. BK20141167), and the Open Project for the State Key Laboratory of Functional Materials for Informatics (No. SKL201507). The authors would like to appreciate the technical staff in the department of Chemical and Materials Engineering for various supports. We also want to express our gratitude to Mr Glen Slater, Mr Chris Goode and technical staff in Rigg Electroplating Ltd.

References

1. K. K. Arunsunai, K. G. Paruthimal and V. S. Muralidharan, *Appl. Surf. Sci.*, 259 (2012) 231.
2. A. A. Aal, M. Bahgat and M. Radwan, *Surf. Coat. Tech.*, 201(2006)2910.
3. M. Crobu, A. Scorciapino, B. Elsener, A. Rossi, *Electrochim. Acta.*, 53 (2008) 3364.
4. S. R. Allahkaram, S. Golroh and M. Mohammadalipour, *Mater. Des.*, 32(2011)4478.
5. X.T. Yuan, D. B. Sun, H. Y. Yu, H. M. Meng, *Appl. Surf. Sci.*, 255(2009) 3613.
6. R.A. Shakoor, Ramazan Kahraman, Umesh Waware, Yuxin Wang, Wei Gao, *Mater. Des.*, 64(2014)127.
7. C.F. Malfatti, H.M. Veit, T.L. Menezes, J. Zoppas Ferreira, J. S. Rodrigues, J. P. Bonino, *Surf. Coat. Technol.*, 201 (2007) 6318.
8. 9. Y. d. Hazan, D. Zimmermann, M. Z'graggen, S. Roos, C. Aneziris, H. Bollier, P. Fehr, T. Graule, *Surf. Coat. Technol.*, 204 (2010) 3464.
9. K. Krishnaveni, T.S.N. Sankara Narayanan, S.K. Seshadri, *Mater. Chem. Phys.*, 99(2006) 300.
10. P. Gyftou, E.A. Pavlatou and N. Spyrellis, *App. Surf. Sci.*, 254 (2008) 5910.
11. Jan Steinbach and Hans Ferkel, *Scripta Mater.*, 44 (2001) 1813.
12. K. K. Arunsunai, P. Mohan, K. G. Paruthimal, and V. S. Muralidharan, *J. Nanosci. Nanotechnol.*, 12(2012) 8364.
13. S.A. Lajevardi, and T. Shahrabi: *App. Surf. Sci.*, 256 (2010) 6775.
14. S. Ranjan, D. Siddhartha, D. Karabi, *Metall. Mater. Trans.*, A 43 (2012)3809.
15. N.S. Qu, W.H. Qian, X.Y. Hu, Z.W. Zhu, *Int. J. Electrochem. Sci.*, 8 (2013)11564.
16. S.T. Aruna, C.N. Bindu, V. Ezhil Selvi, V.K. William Grips, K.S. Rajam, *Surf. Coat. Technol.*, 200 (2006) 6871.
17. R. Arghavanian, N.P. Ahmadi, *J. Solid State Electrochem.*, 15 (2011) 2199e2204.

18. V.P. Singh, P.K. Tikoo, *J. Appl. Electrochem.* 8 (1978) 41.
19. S. Kasturibai a, b, G. Paruthimal Kalaiganan, *Mater. Chem. Phys.* 147(2014)1042.
20. K. H. Hou, W. H. Hwu, S. T. Ke, M. D. Ger, *Mater. Chem. Phys.* 100 (2006) 54.
21. P.-A. Gay, J.M. Limat, P.A. Steinmann, and J. Pagetti, *Surf. Coat. Technol.* 202 (2007) 1167.
22. Y. Yang and Y.F. Cheng: *Surf. Coat. Technol.* 216 (2013) 282.
23. W. Sassi, L. Dhouibi, P. Berçot, M. Rezrazi and E. Triki, *Surf. Coat. Technol.* 206 (2012) 4235.

© 2016 The Authors. Published by ESG (www.electrochemsci.org). This article is an open access article distributed under the terms and conditions of the Creative Commons Attribution license (<http://creativecommons.org/licenses/by/4.0/>).